



An improved model for predicting elemental sulphur saturation in sour gas reservoir with incidence of reservoir compaction

Adesina Fadairo, Oladele Omodara & Churchill Ako

To cite this article: Adesina Fadairo, Oladele Omodara & Churchill Ako (2018) An improved model for predicting elemental sulphur saturation in sour gas reservoir with incidence of reservoir compaction, Geosystem Engineering, 21:1, 53-60, DOI: [10.1080/12269328.2017.1379447](https://doi.org/10.1080/12269328.2017.1379447)

To link to this article: <https://doi.org/10.1080/12269328.2017.1379447>



Published online: 24 Sep 2017.



Submit your article to this journal [↗](#)



Article views: 26



View related articles [↗](#)



View Crossmark data [↗](#)



An improved model for predicting elemental sulphur saturation in sour gas reservoir with incidence of reservoir compaction

Adesina Fadairo, Oladele Omodara and Churchill Ako

Department of Petroleum Engineering, Covenant University, Ota, Nigeria

ABSTRACT

Elemental sulphur which is originally soluble in gas phase in the reservoir should precipitate from the gas phase after exceeding saturation state and deposit at pore spaces and throat sequentially resulting in porosity and permeability loss. Over several decades, modelling elemental sulphur deposition around the wellbore are mainly focused on the gas reservoir and were based on Darcy flow. Few recent studies have shown models that capable for predicting elemental sulphur deposition considered non-Darcy flow, variations in gas properties with pressure change as well as permeability reduction caused by compaction. It therefore follows that if compaction causes a reduction in the permeability of the reservoir as well as reduction in its porosity, then porosity damage function induced by compaction becomes a crucial factor needed to be incorporated into the existing models to adequately predict sulphur saturation. This study is concerned with developing an accurate model for predicting elemental sulphur saturation in the fractured reservoir by exploring the functional relationship between compaction and elemental sulphur deposition over time. The result obtained from newly improved model is at variance with that obtained from Guo et al. model. This variance may not be unconnected with the fact that the rate of sulphur deposition seemed to have been underestimated by Guo et al. model. The refined model is more accurate and practical in predicting sulphur deposition in fractured sour gas reservoir as it leads to a faster rate of sulphur deposition.

ARTICLE HISTORY

Received 15 August 2017

Accepted 10 September 2017

KEYWORDS

Elemental sulphur; compaction; sour gas reservoir; permeability loss function; porosity loss function

Introduction

The problem of elemental sulphur deposition has been mainly covered in the areas of chemical engineering, gas processing and chemical analysis (Flowers, 1990; Sung & Jonshon, 1989). The proposed treatments were chemical separation or biological and microbial treatments (Gasiorek, 1994; Ruitenberg, Dijkman, & Buisman, 1999). On the other hand, elemental sulphur is more often than not, present in appreciable quantities in sour gas under reservoir conditions (Brunner, Place, & Woll, 1988; Brunner & Woll, 1980). A large number of research studies concentrated on sulphur deposition, especially of gas reservoirs, have been carried out and a lot of recognition of problems owing to sulphur deposition associated with the production of sour gas has been achieved. Sulphur precipitation can impair well productivity and the economics of reserve depletion (Brunner & Woll, 1980; Kuo, 1972). Kuo (1972) developed the first mathematical model of a solid-phase precipitation in porous media and its influence on fluid flow. The model considered elemental

sulphur as some of the dissolved sulphur precipitate from the solution as a result of depletion of reservoir pressure. The results of the study showed a rapid build up of solid sulphur around the well and significant depositions near the outer boundary of the reservoir. Roberts (1997) built the empirical formula proposed by Chrastil (1982) and the experimental data of Brunner and Woll (1980); Brunner et al. (1988) for a convectional black oil reservoir simulator to model sulphur depositional processes and described significant flow impairment induced by sulphur deposition for a history match of the Waterton field case.

Porosity damage was introduced into Roberts model by Fadairo, Ako, and Falode (2012). Further enhancements to Roberts model were introduced by Mahmoud and Al-Majed (2012) where deviation factor, gas volume factor, and viscosity were addressed as a function of pressure. Hands, Oz, Roberts, and Davis (2002) researched the effect of natural fracture on sulphur deposition and Hu, He, Wang, Zhao, and Dong (2013) developed a mathematical model of sulphur deposition damage in the presence

of natural fracture, but the model did not demonstrate the effect of fracture on the formation permeability. Few recent studies have shown models that capable for predicting elemental sulphur deposition considered non-Darcy flow, variations in gas properties with pressure change as well as permeability reduction caused by compaction. It therefore follows that if compaction causes a reduction in the permeability of the reservoir as well as reduction in its porosity, then it becomes a crucial factor needed to be incorporated into the existing model to adequately predict sulphur saturation. This idea was neglected by all the previous models.

This study is concerned with developing a more accurate model for the prediction of elemental sulphur saturation in the fractured reservoir by exploring the functional relationship between compaction and elemental sulphur deposition over time.

Prediction model of sulphur solubility

Experimental determination of the solubility of sulphur in a specific reservoir fluid is a task that is very cumbersome, costly and time consuming. Hence, sulphur solubility prediction model and a predictive technique for adequately estimating sulphur solubility in sour gas is crucial for sulphur precipitation. To empirically predict elemental sulphur critical temperature and pressure in sour gas reservoir development, Chrastil (1982), employed the principle of thermodynamics based on associative law and entropy to model an empirical solubility equation that is extensively used for predicting the solubility of elemental sulphur in fluid under high pressure.

The mathematical expression is represented as:

$$C_r = \rho^k e^{\left(\frac{M}{T} + N\right)} \quad (1)$$

where C_r is the solubility of the solid-phase sulphur (g/cm^3), ρ is the fluid density (kg/m^3), T is temperature (K), and k , M and N are empirical constants which can be obtained by experimental data regression.

A typical empirical equation analogous to Equation (1) for sulphur solubility in sour gas mixture is obtained using experimental data reported by Roberts (1997) is as follows:

$$C = \rho^4 e^{\left(-\frac{4666}{T} - 4.5711\right)} \quad (2)$$

where C is the solubility of sulphur.

In a specific sour gas reservoir, pressure and temperature remain the paramount parameters that control the solubility of sulphur, as gas flow in porous media in the formation is considered as an isothermal process. Hence, the reservoir pressure is the key factor controlling sulphur deposition in pay zones.

The fluid density in Equation (2) can be calculated as:

$$\rho = \frac{M_a \gamma_g P}{ZRT} \quad (3)$$

Differentiating Equation (2) with respect to pressure

$$\frac{dC}{dP} = 4P^3 \left(\frac{M_a \gamma_g}{ZRT} \right)^4 \exp\left(-\frac{4666}{T} - 4.5711\right) \quad (4)$$

In Equation (4), $\frac{dC}{dP}$ is a cubic function of pressure and changes dramatically in the zone near the wellbore.

where M_a is the molecular weight of air = 28.97; γ_g is gas relative density; R is universal gas constant; T is the formation temperature, K; Z is the gas deviation – factor; P is the gas reservoir pressure, MPa.

Model development

The following assumptions were made in order to formulate and solve the mathematical model:

- (1) Non-Darcy flow and constant temperature and production rate
- (2) The reservoir fluid is saturated with elemental Sulphur
- (3) Sulphur is saturated in the gas phase in the formation
- (4) Low permeability shale gas formation with nano-sized pores

Prediction model of sulphur saturation

The radial steady flow model is illustrated in Figure 1.

The volume of sulphur that drops in the pore over a given time interval (Robert 1997), is given as;

$$dV_s = \frac{q_g B_g \left(\frac{dC}{dP} \right) dP}{\rho_s} dt \quad (5)$$

where V_s is precipitated sulphur volume, m^3 ; ρ_s is the density of sulphur, $2.07 \text{ g}/\text{cm}^3$; t is production time, days.

Sulphur saturation in porous media S_s is defined as the ratio of the volume of the deposited sulphur to the pore volume at the radial distance dr :

$$dS_s = \frac{dV_s}{2\pi r h \phi_i (1 - S_{wi}) dr} \quad (6)$$

The flow in the vicinity of the wellbore is non-Darcy flow which can be described as

$$\frac{dP}{dr} = \frac{\mu_g}{k} v + \beta \rho_g v^2 \quad (7)$$

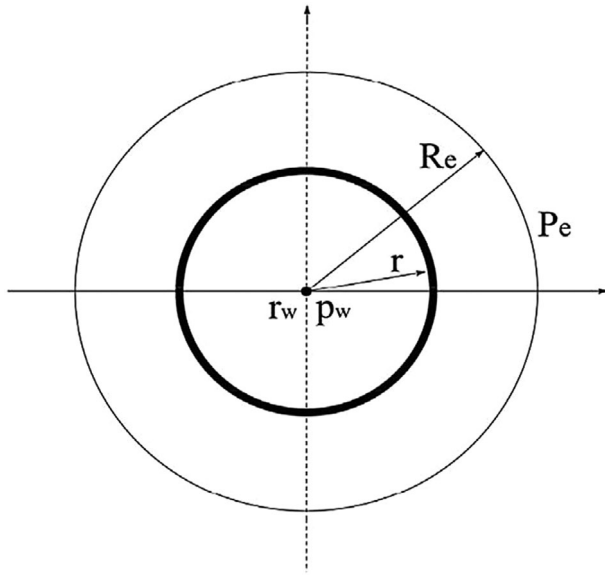


Figure 1. A pictorial representation of two-dimensional radial flow.

Combining Equations (4), (5) and (7) we have:

$$\frac{dS}{dt} = 7.69 \times 10^{-4} \times \left[\frac{\mu_g q_g B_g (dC/dP)}{rh\phi k k_{rg} (1 - S_{wi})} v + \frac{\beta \rho_g q_g B_g (dC/dP)}{rh\phi (1 - S_{wi})} v^2 \right] \quad (8)$$

where;

$$v = \frac{1.157 \times 10^{-5} q_g B_g}{2\pi rh} \quad (9)$$

$$\beta = \frac{7.644 \times 10^{10}}{k_c^{\frac{3}{2}}} \quad (10)$$

Substituting Equations (9) and (10) into Equation (8)

$$\frac{dS}{dt} = 1.417 \times 10^{-4} \left[\frac{\mu_g q_g^2 B_g^2 \left(\frac{dc}{dp} \right)}{r^2 h^2 \phi (k_g) (1 - s_{wi})} \right] + 2.0 \times 10^{-14} \left[\frac{\rho_g q_g^3 B_g^3 \left(\frac{dc}{dp} \right)}{r^3 h^3 \phi (k_g)^{1.5} (1 - s_{wi})} \right] \quad (11)$$

Here we introduce the empirical relationship between the relative permeability of the gas phase and the sulphur saturation proposed by Kuo (1972), as

$$k_{rg} = e^{\alpha S_s} \quad (12)$$

Civan et al. (1989) expressed the relationship between the ratio current to original permeability as function of blocked porosity as

$$\frac{k}{k_i} = \left(\frac{\phi}{\phi_i} \right)^m \quad (13)$$

Fadairo and Ako (2010) proposed porosity damage function due to precipitation of elemental sulphur by incorporating the above relative permeability function given by Kuo (1972) into the permeability–porosity relationship given by Civan et al. (1989) and derive a relationship between initial porosity ϕ_0 , instantaneous porosity ϕ_i and the elemental sulphur saturation.

$$\phi = \phi_i e^{\frac{\alpha S_s}{m}} \quad (14)$$

where S_s is sulphur saturation; ϕ is the porosity of gas reservoir at any location; ϕ_i is the initial porosity of gas reservoir; α and m are empirical constants which can be obtained experimentally.

For a high sulphur content-fractured reservoir, stress-induced permeability reduction can be expressed in the following equation which is a relationship that relates permeability to compaction (Guo, Zhou, & Zhou, 2015)

$$k = k_i e^{-\lambda(P_i - P)} \quad (15)$$

Where λ is the permeability modulus and it is used to characterize the degree of permeability stress-sensitivity. P_i is the initial pressure, P is the current pressure, k_i is the permeability at the initial pressure, and k is the permeability at the current pressure.

Substituting Equation (15) into (13)

$$\frac{k_i e^{-\lambda(P_i - P)}}{k_i} = \left(\frac{\phi}{\phi_i} \right)^m \quad (16)$$

We obtain another relationship that relates porosity to compaction as:

$$\phi = \phi_i e^{\left(\frac{-\lambda(P_i - P)}{m} \right)} \quad (17)$$

Combining Equations (12), (14), (15) and (17)

$$(\phi k_g)^2 = (\phi_i k_i)^2 e^{\alpha S_s - \lambda \Delta P + \frac{\alpha S_s}{m} - \frac{\lambda \Delta P}{m}} \quad (18)$$

Hence,

$$\phi k_g = \phi_i k_i \sqrt{e^{\alpha S_s - \lambda \Delta P + \frac{\alpha S_s}{m} - \frac{\lambda \Delta P}{m}}} \quad (19)$$

Substituting Equation (19) in (11)

$$\frac{dS_s}{dt} = 1.417 \times 10^{-4} \times \left[\frac{\mu_g q_g^2 B_g^2 \left(\frac{dc}{dp} \right)}{r^2 h^2 (1 - s_{wi}) \theta_i k_i \sqrt{e^{\alpha S_s - \lambda \Delta P + \frac{\alpha S_s}{m} - \frac{\lambda \Delta P}{m}}}} \right] + 2.0 \times 10^{-14} \times \left[\frac{\rho_g q_g^3 B_g^3 \left(\frac{dc}{dp} \right)}{r^3 h^3 (1 - s_{wi}) \theta_i k_i \sqrt{e^{1.5 \alpha S_s - 1.5 \lambda \Delta P + \frac{\alpha S_s}{m} - \frac{\lambda \Delta P}{m}}}} \right] \quad (20)$$

In order to simplify the equation we assign

$$A = \frac{6.78 \times 10^{-11} \mu_g q_g^2 (M_a \gamma_g)^4 e^{\left(\frac{-4666}{T} - 4.5711 \right)}}{Z^2 R^4 T^2 r^2 h^2 (1 - S_{wi}) \theta_i k_i} \quad (21)$$

$$B = \frac{3.31 \times 10^{-24} q_g^3 (M_a \gamma_g)^5 e^{\left(\frac{-4666}{T} - 4.5711 \right)}}{Z^2 R^5 T^2 r^3 h^3 (1 - S_{wi}) \theta_i k_i^{1.5}} \quad (22)$$

Therefore

$$\frac{dS_s}{dt} = \frac{A}{\sqrt{e^{\alpha S_s - \lambda \Delta P + \frac{\alpha S_s}{m} - \frac{\lambda \Delta P}{m}}}} + \frac{B}{\sqrt{e^{1.5 \alpha S_s - 1.5 \lambda \Delta P + \frac{\alpha S_s}{m} - \frac{\lambda \Delta P}{m}}}} \quad (23)$$

Evaluating Equation (23), we have:

$$\frac{dt}{dS_s} = \frac{\left(e^{1.5 \alpha S_s - 1.5 \lambda \Delta P + \frac{\alpha S_s}{m} - \frac{\lambda \Delta P}{m}} \right)^{0.5}}{\left[A e^{0.25 \alpha S_s - 0.25 \lambda \Delta P} + B \right]} \quad (24)$$

$$\text{Let } a = e^{-0.5 \lambda (p_i - p)} = \left(\frac{k}{k_i} \right)^{0.5} \quad (25)$$

Inserting equation (25) into (24) and solve, we have

$$\text{Hence } \frac{dt}{dS_s} = \frac{\left(a^3 e^{1.5 \alpha S_s + \frac{\alpha S_s}{m} - \frac{\lambda \Delta P}{m}} \right)^{0.5}}{A a^{0.5} e^{0.25 \alpha S_s} + B} \quad (26)$$

Evaluating equation (26) further

$$\frac{dt}{dS_s} = \frac{a}{A} \left(\frac{e^{0.75 \alpha S_s + \frac{0.5 \alpha S_s}{m} - \frac{0.5 \lambda \Delta P}{m}}}{e^{0.25 \alpha S_s} + \frac{B}{A a^{0.5}}} \right) \quad (27)$$

Applying the general assumption, taking $m = 3$ and $\alpha = -6.22$

$$\frac{dt}{dS_s} = \frac{a}{A} \left[\frac{e^{\frac{2.75 \alpha S_s}{3} - \frac{0.5 \lambda \Delta P}{3}}}{e^{0.25 \alpha S_s} + \frac{B}{A a^{0.5}}} \right] \quad (28)$$

$$\text{Let } b = e^{-\frac{\lambda \Delta P}{3}} = e^{-0.33 \lambda \Delta P} \quad (29)$$

Hence the equation for relating sulphur saturation with time is given as:

$$dt = \frac{ab^{0.5}}{A} \left[\frac{e^{0.9233 \alpha S_s}}{e^{0.25 \alpha S_s} + \frac{B}{A a^{0.5}}} \right] dS_s \quad (30)$$

Therefore

$$t = \frac{ab^{0.5}}{A} \int_0^{S_s} \left[\frac{e^{0.9233 \alpha S_s}}{e^{0.25 \alpha S_s} + \frac{B}{A a^{0.5}}} \right] dS_s \quad (31)$$

For Darcy flow when $B = 0$

$$t = \frac{ab^{0.5}}{A} \int_0^{S_s} \left[e^{(0.9233 \alpha S_s - 0.25 \alpha S_s)} \right] dS_s \quad (32)$$

Integrating with respect to S_s we finally obtained the relationship that relate time and saturation under Darcy flow state while also accounting for porosity and permeability damage effects of compaction.

$$t = \frac{ab^{0.5}}{A} \int_0^{S_s} \left[e^{(0.6733 \alpha S_s)} \right] dS_s \quad (33)$$

Calculation of the gas deviation factor (Z-Factor) and gas viscosity

With regard to gas reservoirs with high sulphur content, the deviation factor Z can be obtained by the DPR method Dranchuk, Purvi and Robinson and calibrated by the Wicher and Aziz method (W-A) and is expressed as:

$$Z = 1 + \left(A_1 + \frac{A_2}{T_r} + \frac{A_3}{T_r^3} \right) \rho_{pr} + \left(A_4 + \frac{A_5}{T_r} \right) \rho_{pr}^2 + \frac{A_6}{T_r} + \frac{A_7}{T_r^3} \left(1 + A_8 \rho_{pr}^2 \right) \rho_{pr}^2 e^{(-A_8 \rho_{pr}^2)} \quad (34)$$

where ρ_{pr} is the pseudo relative density defined as;

$$\rho_{pr} = 0.27 \left(\frac{P_{pr}}{Z T_r} \right) \quad (35)$$

where the constants of the DPR model are shown in Table 1.

Table 1. Constants in DPR model used in Z-factor correlation.

A1	A2	A3	A4	A5	A6	A7	A8
0.31506237	-1.0467099	-0.5783273	0.53530771	-0.61232032	-0.10488813	0.68157001	0.68446549

For sour gas reservoirs, considering some common polar molecules (H_2S , CO_2), parameter ϵ is introduced by Wicher-Aziz as report in Guo et al. (2014) which is described as

$$\epsilon = 15(M - M^2) + 4.167(N^{0.5} - N^2) \quad (36)$$

where M is the total mole fraction of H_2S and CO_2 , and N_2 is the mole fraction of H_2S .

The critical temperature and pressure of each component are related to parameter ϵ . The calibration relationship is:

$$T'_{ci} = T_{ci} - \epsilon \quad (37)$$

$$P'_{ci} = \frac{P_{ci} T'_{ci}}{T_{ci}} \quad (38)$$

where T_{ci} is the critical temperature of component i , K ; P_{ci} is the critical pressure of component i , MPa; T'_{ci} is the correction of the critical temperature of component i , K ; P'_{ci} is the correction of the critical pressure of component i , MPa.

The gas viscosity is calculated using Dempsey's model and is corrected by Standing's method, by Dempsey derived a formula, to calculate gas viscosity by matching the plate drawn by Carr And is expressed as:

$$\begin{aligned} \ln \frac{\mu_g}{\mu_1} T_r = & A_0 + A_1 P_r + A_2 P_r^2 + A_3 P_r^3 \\ & + T_r (A_4 + A_5 P_r + A_6 P_r^2 + A_7 P_r^3) \\ & + T_r^2 (A_8 + A_9 P_r + A_{10} P_r^2 + A_{11} P_r^3) \\ & + T_r^3 (A_{12} + A_{13} P_r + A_{14} P_r^2 + A_{15} P_r^3) \end{aligned} \quad (39)$$

$$\begin{aligned} \mu_1 = & \left(1.709 \times 10^{-5} - 2.062 \times 10^{-6} \gamma_g (1.8T + 32) \right. \\ & \left. + 8.188 \times 10^{-3} - 6.15 \times 10^{-3} \log(\gamma_g) \right) \end{aligned} \quad (40)$$

Table 2. The constants for the gas viscosity correlation.

A0	A1	A2	A3
-2.4621182	2.971547	-0.28626	0.008054
A4	A5	A6	A7
2.080861	-3.49803	0.360372	-0.01044
A8	A9	A10	A11
-0.79339	1.396433	-0.14914	0.00441
A12	A13	A14	A15
0.083939	-0.18649	0.020337	-0.000609579

where A0–A15 are constants are tabulated in Table 2 below, μ_1 is the viscosity of the single component under 1 atm (mPa.s), μ_g is the gas viscosity (mPa.s), P_r and T_r are pseudo-reduced pressure and temperature, respectively

Standing's corrected formula is given by:

$$\mu_1 = (\mu_1)_{un} + \mu_{N_2} + \mu_{CO_2} + \mu_{H_2S} \quad (41)$$

where μ_{H_2S} is the corrected viscosity of H_2S , mPa.s; μ_{CO_2} is the corrected viscosity of CO_2 , mPa.s; μ_{N_2} is the corrected viscosity of N_2 , mPa.s; $(\mu_1)_{un}$ is the viscosity of hydrocarbon gas, mPa.s; μ_1 is the corrected viscosity of the hydrocarbon gas using the non-hydrocarbon correction method, mPa.s.

Model validation

Comparing results obtained from the Guo et al. model and the refined model;

Guo et al. model:

$$t = \frac{a^2}{Ap} \int_0^{S_s} \left[\frac{e^{0.9233\alpha S_s}}{e^{0.25\alpha S_s} + \frac{B}{Aa^{0.5}}} \right] dS_s \quad (42)$$

The refined model:

$$t = \frac{ab^{0.5}}{Ap} \int_0^{S_s} \left[\frac{e^{0.9233\alpha S_s}}{e^{0.25\alpha S_s} + \frac{B}{Aa^{0.5}}} \right] dS_s \quad (43)$$

The introduction of the constant b justified in the previous chapter is to account for the impact of porosity change with compaction on deposition of sulphur

where;

$$a = e^{-0.5\lambda(P_i - P)} = \left(\frac{k}{k_i} \right)^{0.5} \quad (44)$$

$$b = e^{-0.33\lambda\Delta P} \quad (45)$$

$$A = \frac{6.78 \times 10^{-11} \mu_g q_g^2 (M_a \gamma_g)^4 e^{\left(\frac{-4666}{T} - 4.5711\right)}}{Z^2 R^4 T^2 r^2 h^2 (1 - S_{wi}) \phi_i k_i} \quad (46)$$

$$B = \frac{3.31 \times 10^{-24} q_g^3 (M_a \gamma_g)^5 e^{\left(\frac{-4666}{T} - 4.5711\right)}}{Z^2 R^5 T^2 r^3 h^3 (1 - S_{wi}) \phi_i k_i^{1.5}} \quad (47)$$

The model is resolved by integrating numerically to obtain the tables and charts below:

Discussion of results

The effects of porosity change with compaction on magnitude of elemental sulphur deposition near the wellbore in a gas reservoir has been estimated and analyzed using the data of the Oilfield presented by (Guo et al., 2014) in their paper as reported in Table 3.

It was observed in Figure 2 that reservoir with incidence of strong compaction at approximately 368 days the Guo et al. model shows a saturation of 0.3 while the refined model shows the same saturation at 345 days. Hence the Guo et al. model by neglecting the porosity change due to compaction underestimated the rate of sulphur deposition in the reservoir over time. It was revealed that inclusion of porosity damage function that arises due to compaction when modelling elemental sulphur saturation in sour gas-fractured reservoir with incidence of compaction may result to higher damage around the gas wellbore.

It was also observed in Figure 3 that when there is weak compaction in the reservoir the Guo model shows a saturation of 0.3 at 432 days while the refined model shows the same saturation at an earlier time (426 days). This shows that the higher the magnitude of compaction in the reservoir, the earlier the blockage time period induced by elemental sulphur in sour gas-fractured reservoir. The result obtained from the figure implies that the weak compaction promotes less elemental sulphur-induced flow impairment in such unconventional reservoir.

Figure 4 shows that if there no compaction in sour gas reservoir Guo et al. model and the modified model record the same results. At approximately 450 days, both models considered in the paper gave saturation of 0.3. This is because no compaction is considered and porosity and permeability change due to compaction in the two considered models in this paper is equal to zero. Avoiding reservoir compaction in fractured reservoir increase the cumulative production of gas prior to the blockage time

Table 3. Parameters used in solving the model.

Parameters	Values	Parameters	Values
Z factor	0.95	R	8.314
Viscosity (Pa.s)	0.00110707	r (m)	1
Initial Pressure (Pa)	36600000	Flow rate (m ³ /day)	200000
BHP (Pa)	10000000	Ma	29
Initial porosity	0.04	Specific gravity	0.72
Temp (K)	361.95	Alpha	-6.22
H (m)	30	Density	1.564624378
Swi	0	Pi-Pwf	26600000
Ka	1	Lander weak	3.06932E-09
Ki	0.000007	Lander strong	1.49211E-08
T_{pr}	1.49	Lander at no compaction	0
P_{pr}	8.03		

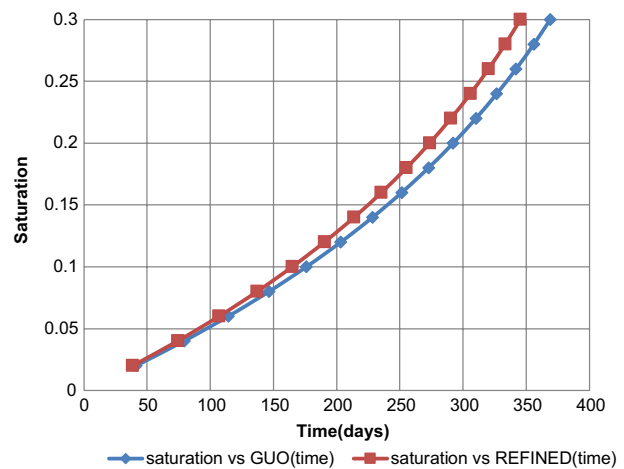


Figure 2. The effect of strong compaction on sulphur saturation.

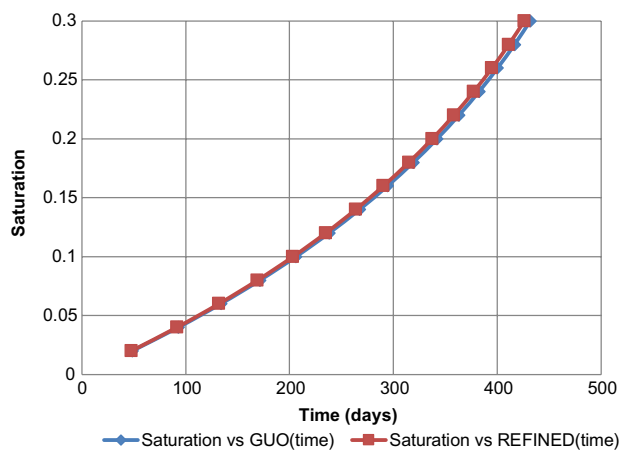


Figure 3. Comparing the result obtained from the Guo Model and the Modified Model when considering weak compaction.

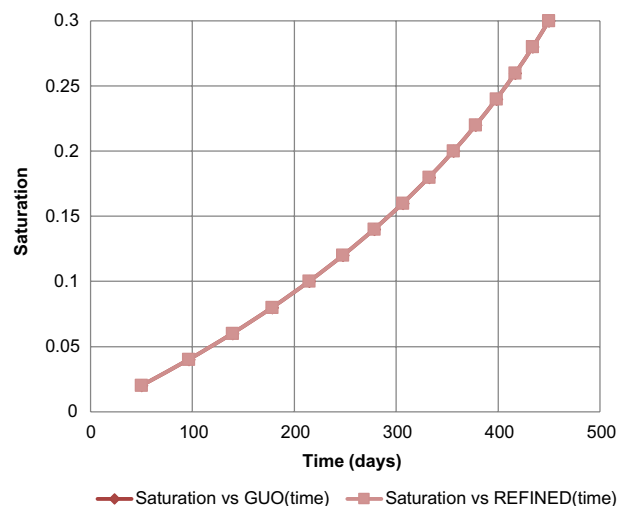


Figure 4. The effect of no compaction on sulphur saturation.

Figure 5 demonstrated the impact of different compaction types on the magnitude of elemental sulphur deposition in the sour gas reservoir. It was observed from the figure that as the degree of compaction increases, the rate of sulphur deposition increases while at constant

saturation, the time decreases. A saturation of 0.3 was obtained at 450 days under no compaction, the same saturation was observed at 426 days under weak compaction and 345 days under strong compaction. This implies that as the intensity of reservoir compaction

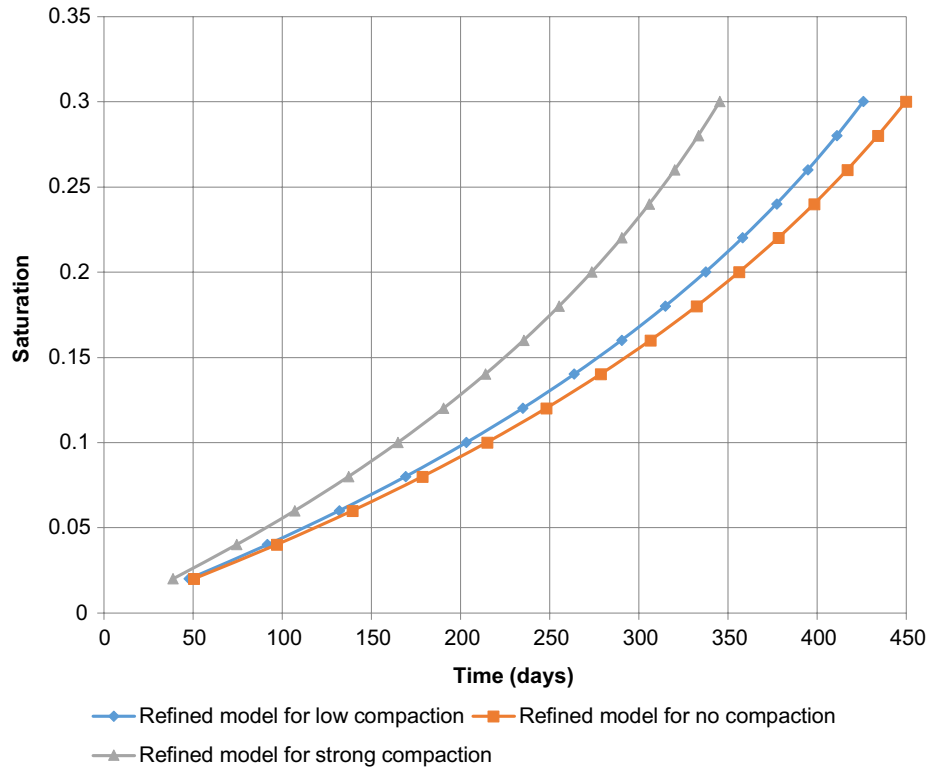


Figure 5. The effect of compaction type on sulphur saturation.

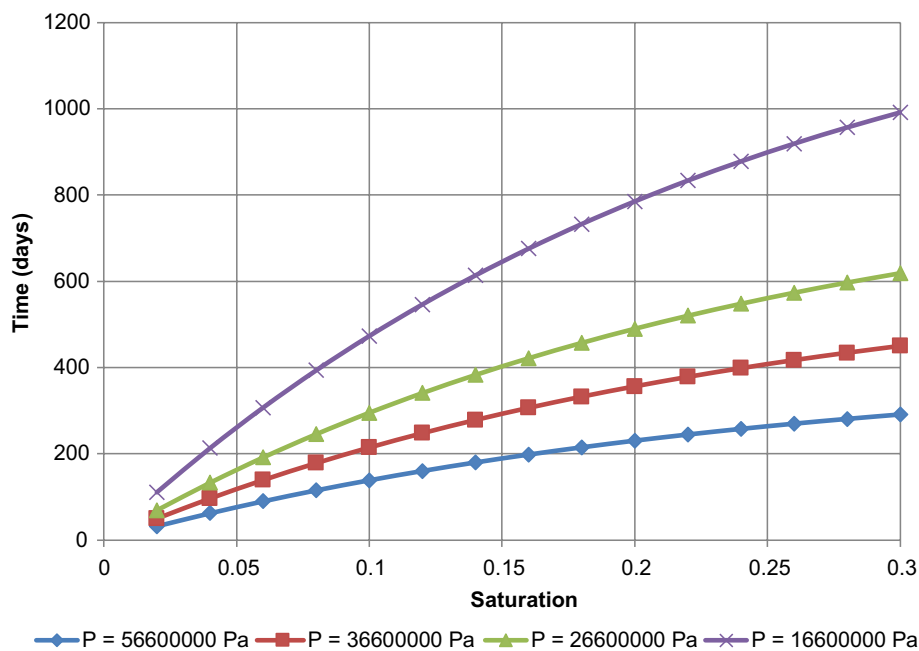


Figure 6. The effect of varied pressure on sulphur deposition under no compaction.

increases, the magnitude of elemental sulphur deposition increases.

Figure 6 also demonstrated that the higher the pressure in the reservoir the faster the rate of elemental sulphur deposition. A sulphur saturation of 0.3 was observed at 992 days at the relatively low pressure of 16600 KPa while the same saturation is observed at 291 days at a pressure of 56600 KPa. Thus, we can conclude that the reservoir pressure drop has a great effect on the amount of sulphur deposited in the reservoir.

Conclusion

Validation of the improved model shows that there is a discrepancy between Guo's Model and the established refined model which suggest that the rate of sulphur deposition seem to have been underestimated by Guo et al. model.

The refined model, considering non-Darcy flow, reservoir compaction and the permeability damage as well as porosity damage function caused by compaction, is more accurate and practical in predicting sulphur deposition in fractured sour gas reservoir. Reservoir compaction is a common phenomenon which should be considered in sulphur deposition prediction, as it leads to a faster rate of deposited sulphur.

Acknowledgement

The authors would like to acknowledge the management of Covenant University for their financial support and thank the management of FatherHerz Forte Technology Nigeria Limited for their technical input towards the successful completion of this work.

Disclosure statement

No potential conflict of interest was reported by the authors.

References

- Chrastil, J. (1982). Solubility of solids and liquids in supercritical gases. *Journal of Physical Chemistry*, 86, 3016–3021.
- Civan, F., Knapp, R., & Ohen, H. (October 1989). Alteration of permeability by fine particle processes. *Journal of Petroleum Science and Engineering*, 3, 65–79.

- Brunner, E., Place, Jr., M. C., & Woll, W. H. (1988). Sulphur solubility in sour gas. *Journal of Petroleum Technology*, 40, 1587–1592.
- Brunner, E., & Woll, W. H. (1980). Solubility of sulphur in hydrogen sulfide and sour gases. *Society of Petroleum Engineers Journal*, 20, 377–384.
- Fadaïro, A., & Ako, C. (2010). Prediction of elemental sulphur saturation around the wellbore. *Global Journal of Researches in Engineering*, 10, 31–37.
- Fadaïro, A., Ako, C., & Falode, O. (2012). *Elemental sulphur induced formation damage management in sour gas reservoir* (SPE Paper 154980). SPE International Conference on Oilfield Scale, Aberdeen, UK. 30–31.
- Flowers, D. G. (1990). Use of permeation devices in the analysis of sulphur gases by gas chromatography. *Industrial & Engineering Chemistry Research*, 29, 1565–1568.
- Gasiorek, J. (1994). Microbial removal of sulphur dioxide from a gas stream. *Fuel Processing Technology*, 40, 129–138.
- Guo, X., Zhou, X., & Zhou, B. (2015). Prediction model of sulfur saturation considering the effects of non-darcy flow and compaction. *Journal of Natural Gas Science and Engineering*, 18–25.
- Hands, N., Oz, B., Roberts, B., & Davis, P. (2002). Advances in the prediction and management of elemental sulfur deposition associated with sour gas production from fractured carbonate reservoir. *SPE Annual Technical Conference and Exhibition*, 77332, 1–18.
- Hu, J. H., He, S. L., Wang, X. D., Zhao, J. Z., & Dong, K. (2013). The modeling of sulphur deposition damage in the presence of natural fracture. *Petroleum Science and Technology*, 31, 80–87.
- Kuo, C. H. (1972). On the production of hydrogen sulfide-sulphur mixtures from deep formation. SPE 3838-PA. *Journal of Petroleum Technology*, 1142–1146.
- Mahmoud M.A, & Al-Majed, A. (2012). *New model to predict formation damage due to sulfur deposition in sour gas wells* (pp. 20–22). Society of petroleum Engineers. (SPE paper 149535).
- Roberts, B. E. (1997). The effect of sulfur deposition on gaswell inflow performance. *SPE 36707 Reservoir Engineering*, 12, 118–123.
- Ruitenbergh, R., Dijkman, H., & Buisman, C. J. N. (1999). Biologically removing sulphur from dilute gas flows. *Journal of the Minerals Metals & Materials*, 51, 45–45.
- Sung, N. J., & Jonshon, S. J. (1989). Determination of the total amount of sulphur in petroleum fraction by capillary gas chromatography in combination of cold trapping, a total sulphur analyzer. *Journal of Chromatography A*, 468, 345–358.